

## Polypyrrole Films Deposited on Carbon-Steel CS-1018 and Its Interaction with Mexican Crude Oil

Oscar E. Vázquez-Noriega<sup>1</sup>, Javier Guzmán<sup>2,4</sup>, Nohra V. Gallardo-Rivas<sup>1</sup>, Juan Reyes-Gómez<sup>3</sup>, Ana M. Mendoza-Martínez<sup>1</sup>, José L. Rivera-Armenta<sup>1</sup>, Ulises Páramo-García<sup>1,\*</sup>

<sup>1</sup>División de Estudios de Posgrado e Investigación, Instituto Tecnológico de Cd. Madero, Juventino Rosas y Jesús Urueta S/N, Col. Los Mangos, 89440 Cd. Madero, Tamps., MEXICO.

<sup>2</sup>Instituto Mexicano del Petróleo, Eje Central Lázaro Cárdenas, Norte 152, Col. San Bartolo Atepehuacán, 07730 México D.F. MEXICO.

<sup>3</sup>Facultad de Ciencias, Universidad de Colima, Bernal Díaz del Castillo 340, Col. Villas San Sebastián, 28045 Colima, Col., MEXICO

<sup>4</sup>División de Química y Energías Renovables, Universidad Tecnológica de San Juan del Río, Av. de la Palma 125, Col. Vista Hermosa, 76800, San Juan del Río, Querétaro, MEXICO.

\*E-mail: [uparamo@itcm.edu.mx](mailto:uparamo@itcm.edu.mx)

Received: 30 April 2015 / Accepted: 28 May 2015 / Published: 24 June 2015

---

Conductive polymers such as polypyrrole, PPy, are materials capable of conducting electrical current. In this paper two techniques for the electrodeposition of PPy on carbon steel were used: Cyclic Voltammetry (CV) and Chronoamperometry (CA). The characteristics of film electrosynthesized on the carbon-steel substrate (CS-1018) using KNO<sub>3</sub> as supporting electrolyte was studied. The results concluded that under experimental conditions used is possible make a PPy film with adequate characteristics. Important factors were the grip and electrochemical stability of the formed film on steel, which depends on the electrosynthesis technique and in some cases favored by a pretreatment with a 10% HNO<sub>3</sub> solution applied to the steel prior to electropolymerization. The results showed that the polypyrrole deposited with pretreatment completely covered the steel surface and showed better stability and grip.

---

**Keywords:** Conducting polymers, asphaltenes, carbon steel, polypyrrole.

### 1. INTRODUCTION

A common problem in hydrocarbon transportation industry is the formation of scales or solid deposits in pipelines where the product flows. The heaviest oil fraction (asphaltenes) is responsible for this formation, causing a number of problems, mainly pipe clogging and heat exchange deficiencies [1-

6].

There are several methods to prevent and/or remove asphaltenes deposits: mechanical methods [7], chemical cleaning [8, 9], pressure, temperature and flow rate manipulations [10] additives and chemical inhibitors [11, 12].

The conductive polymers applications are highly variable and depend on the synthesis conditions [13-16]. Therefore, it is necessary to carry out electrochemical studies to understand some of the variables that affect the characteristics of PPy electrodeposition on the steel surface (stability, hardness, adhesion, roughness, film size, etc.) [17-22].

When a conductive polymer is attached to a metal surface, this coating can serve as a selective permeable layer (like a membrane). This lets through certain ions or molecules and rejects others, depending on the inter- and intra-molecular arrangement, electronic nature and chemical affinity. Studies related to the conductive polymers stability on steel substrates and corrosion inhibition has been reported [23-25].

In this paper the properties of electrosynthesized polypyrrole on carbon steel 1018 surfaces and its inter-relation with Mexican heavy crude oil were studied, which is a novel application of such polymers. In the best of our knowledge there are no reports in the literature on this research line.

## 2. EXPERIMENTAL SECTION

### 2.1. Chemical reagents

The electrolytes were 0.1 mol L<sup>-1</sup> aqueous solutions of KNO<sub>3</sub> and KCl (J. T. Baker, reagent grade). A 0.1 mol L<sup>-1</sup> Pyrrole (Py, Aldrich) solution was prepared after purification in a bed column packed with silica and activated carbon. All the solutions were prepared with Millipore deoxygenated water (18.2 MΩ) during 15 min with an atmosphere of pure nitrogen (Praxair, 99.99%) before the experiments. The film stability was recorded in a KCl electrolyte with a procedure reported [26].

The oil used comes from the Gulf of Mexico and presents the following characteristics: 15 °API, 25% weight of asphaltenes, density 0.9647 g cm<sup>-3</sup> and a kinematic viscosity of 1,697 mPa s.

### 2.2. Materials

A three electrode cell was used, using as the reference electrode an aqueous saturated calomel electrode, SCE (Tacussel), as the auxiliary electrode graphite and carbon steel, CS-1018, as the working electrode. The CS-1018 is polished manually with different grain sandpaper to obtain a defined surface and it is then subjected to ultrasound (Branson 2510) for 5 min to remove surface contaminants. In order to increase the polymer adhesion on the steel surface is necessary to perform a pretreatment obtaining a higher roughness mordant layer. For which some authors [24, 25] immerse the metal surface in acidic solutions of HCl or HNO<sub>3</sub>. In this study a treatment to the working electrode with 10% HNO<sub>3</sub> was performed with an immersion time of 2 min. Treated surfaces were designated as

treated in HNO<sub>3</sub> (T) and only polished surfaces without acidic treatment were designated as untreated in HNO<sub>3</sub> (NT).

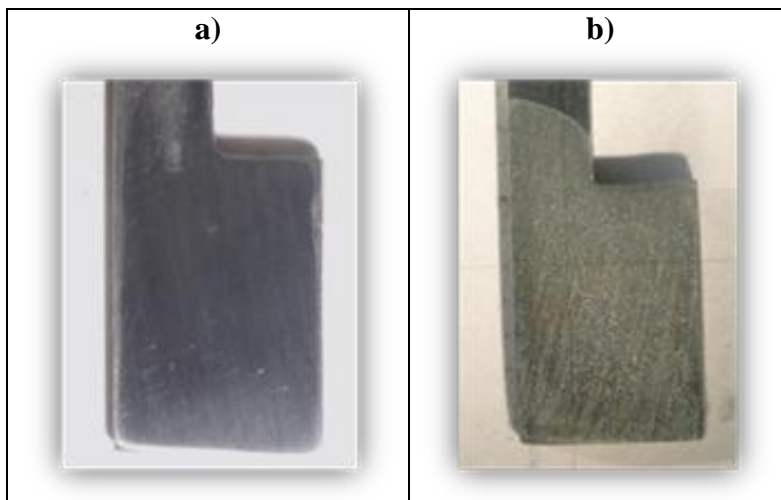


**Figure 1.** Working electrode: a) untreated (NT) and b) treated (T) in 10% HNO<sub>3</sub>.

### 2.3. Equipment

A Gamry Potentiostat Reference-600 was used for electrosynthesis of polypyrrole. A conventional three-electrode cell was used at room temperature ( $20\pm 3^\circ\text{C}$ ). The conditions for the synthesis of PPY films by the cyclic voltammetry technique were: scan rate  $100\text{ mVs}^{-1}$ , initial potential  $-0.8\text{ V/SCE}$ , final potential  $1.0\text{ V/SCE}$  and 40 cycles of polymerization; the conditions for the chronoamperometry method were: constant potential of  $1.0\text{ V/SCE}$  during 300 seconds. For the characterization of the films a scanning electron microscope, SEM (Jeol, JSM-6390LV), which has a X-ray diffraction spectroscopy EDX (Oxford Instruments, INCAx-sight), an Atomic Force Microscope, AFM (Veeco, Innova Scanning Probe Microscope) and an equipment to measure contact angle (Chem Instruments, CAM-plus). The contact angle measurements of the study surfaces were conducted with deionized water and crude oil, in two areas of the sample and three measurements in each zone were taken every 2 min for 10 min. An average value was obtained from these measurements.

## 3. RESULTS AND DISCUSSION

### 3.1. CS-1018 substrate characterization

The Figures 2a and 2c shows the micrographs of the CS-1018 NT substrate obtained by SEM and AFM, respectively, the lines attributed to the mechanical polishing are observed. In Figures 2b and 2d, the CS-1018 T substrate is shown, it is observed that the surface undergoes an attack due to the action of HNO<sub>3</sub>. As can be seen the surface presents different roughness: a)  $R_q = 0.0509\text{ }\mu\text{m}$  b)  $R_q =$

0.739  $\mu\text{m}$ , respectively. This difference in the roughness value will be important for the adhesion effect of the polymeric material to be synthesized on it.

### 3.2. PPy films electrodeposition

Some studies [27] indicate that the synthesis of the polymer on the electrode surface occurs after the saturation of the solution in contact with oligomers. Subsequently, the growth proceeds through the successive addition of monomer units to the deposited polymer chains. Other authors [28] found that the expansion rate of the polymer phase is controlled by the ohmic resistance during growth, suggesting that the growth occurs by slow oxidation of the deposited polymer, followed by the rapid addition of monomers. In this work, the results obtained by two electrochemical techniques are presented, CV and CA.

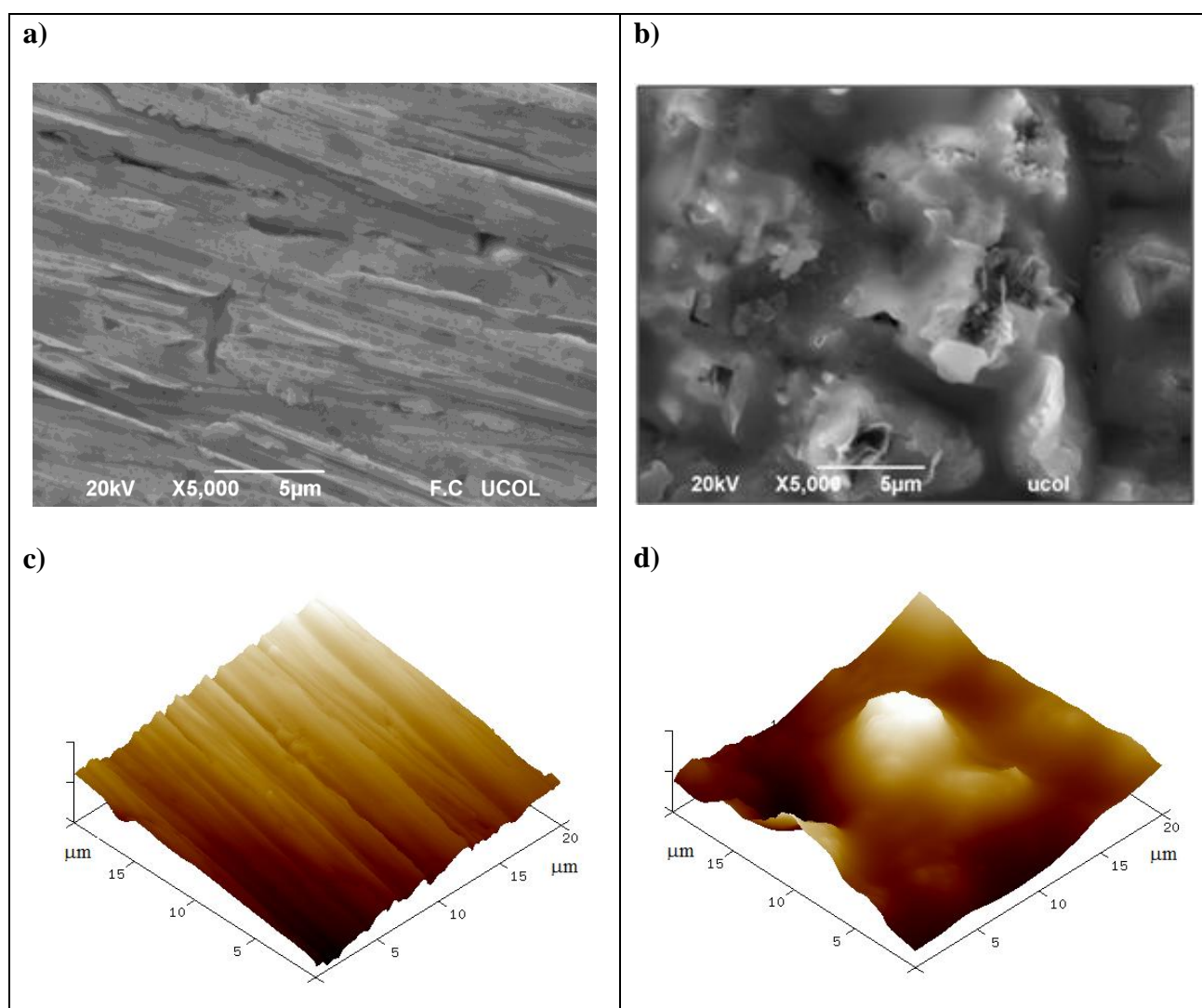


**Figure 2.** SEM and AFM micrographs of CS-1018: a) and c) untreated (NT), b) and d) treated (T) in 10%  $\text{HNO}_3$ .

In Figure 3 shows the cyclic voltammograms of the polymerization of polypyrrole in  $\text{KNO}_3$  with  $\text{Py } 0.1 \text{ mol L}^{-1}$ , on CS-1018 NT and CS-1018 T. Both voltammograms show the irreversible oxidation signal of the Py monomer at an oxidation potential of  $0.9 \text{ V/SCE}$ ; and the charge/discharge zone of the PPy from  $-0.2$  to  $0.7 \text{ V/SCE}$  [29]. An irregular reduction signal is observed from  $-0.1$  to  $-0.8 \text{ V/SCE}$ , which can be attributed to the adsorption process of dopant anion on the substrate surface according to what is reported in the literature [30, 31].

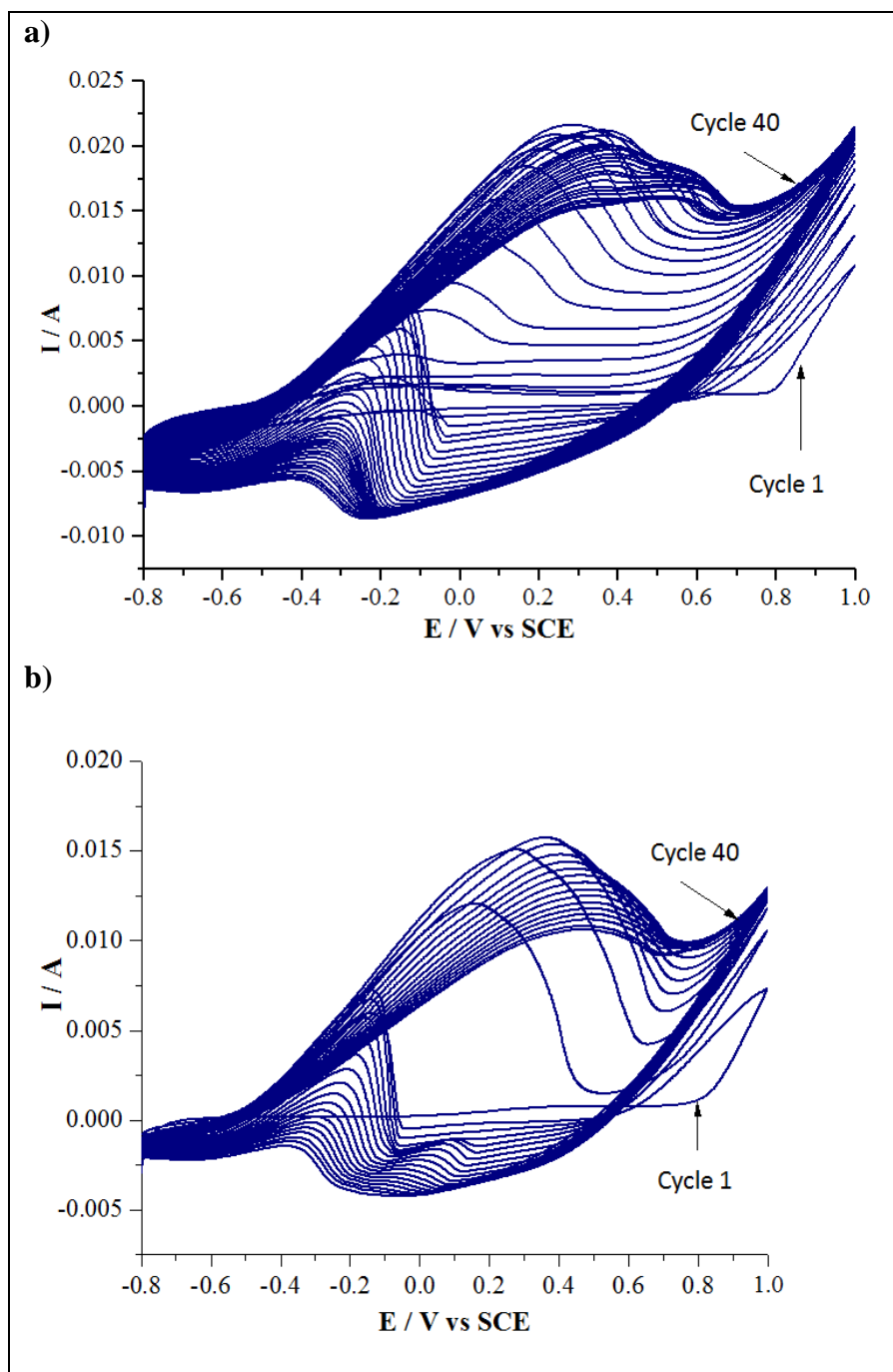


**Figure 3.** Cyclic voltammogram of the PPy formation on CS-1018 surface in a  $\text{KNO}_3$  solution with  $0.1 \text{ mol L}^{-1}$  Py: a) untreated (NT) and b) treated (T) in  $10\% \text{ HNO}_3$ . (40 cycles,  $100 \text{ mVs}^{-1}$ ).

In the Figure 4, the deposition of PPy in  $\text{KNO}_3$  solution is shown when the constant potential method is used as synthesis technique. A slight increase in the current is observed, and therefore an increase in the amount of polymer deposited on the CS-1018 T surface with respect to the CS-1018 NT surface. The electrodeposition in both cases was achieved by applying a constant potential of 1.0 V/SCE for a period of 300 seconds.

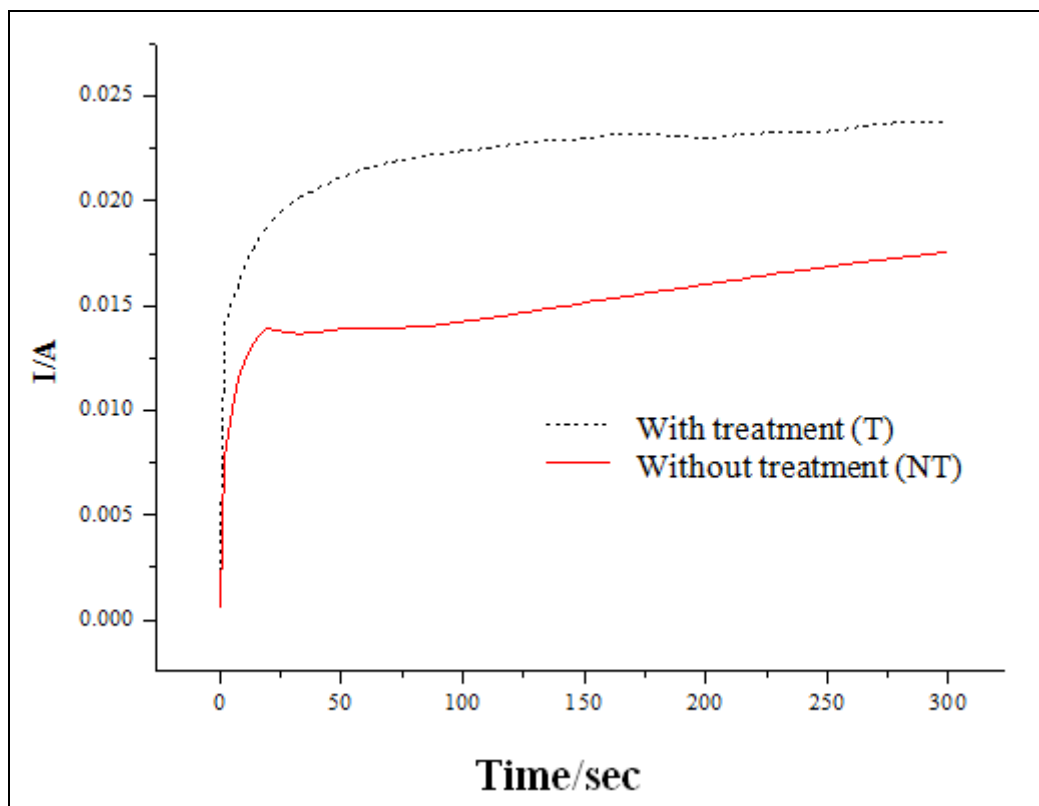


**Figure 4.** Chronoamperogram of PPy formation on CS-1018, in a Py  $0.1 \text{ mol L}^{-1}$  in  $\text{KNO}_3$  solution (1.0 V/SCE,  $t = 300 \text{ s}$ ).

### 3.3. PPy morphology on CS-1018

To perform the morphological study of PPy deposits on CS-1018 SEM and AFM was used. In Figure 5a, the scanning electron micrograph of the PPy deposit obtained by CV in a potassium nitrate solution on the CS-1018 NT surface is shown. It shows a circular or globular clusters morphology, as reported in the literature [32].

In Figure 5b the scanning electron micrograph of PPy synthesized in the same conditions as the 5a but on a treated surface is presented; and an irregular structure deposit is observed, this attributed to the substrate roughness, which affects the morphology of the formed polymer deposit.

Figure 5c shows the atomic force microscopy of PPy deposited on CS-1018 NT where an irregular film can be observed, reaching heights of  $7.62 \mu\text{m}$ . The deposit presents a geometric nodular (semicircular) tendency with superficial dimensions ranging between  $2.23 \mu\text{m}^2$  and  $5.41 \mu\text{m}^2$ . This deposit shows a roughness of  $1.34 \mu\text{m}$ .

In Figure 5d, the atomic force microscopy micrograph of the PPy deposit on CS-1018 T is shown, where the film is not homogeneous, presenting an irregular accommodation because of the morphology of the CS-1018 T surface, reaching heights of  $7.25\ \mu\text{m}$ . It shows circular nodules with a surface area from  $2.43\ \mu\text{m}^2$  to  $6.07\ \mu\text{m}^2$ . The surface roughness of this deposit was  $1.29\ \mu\text{m}$ . The morphologies show a characteristic topography of conductive polymers [32].

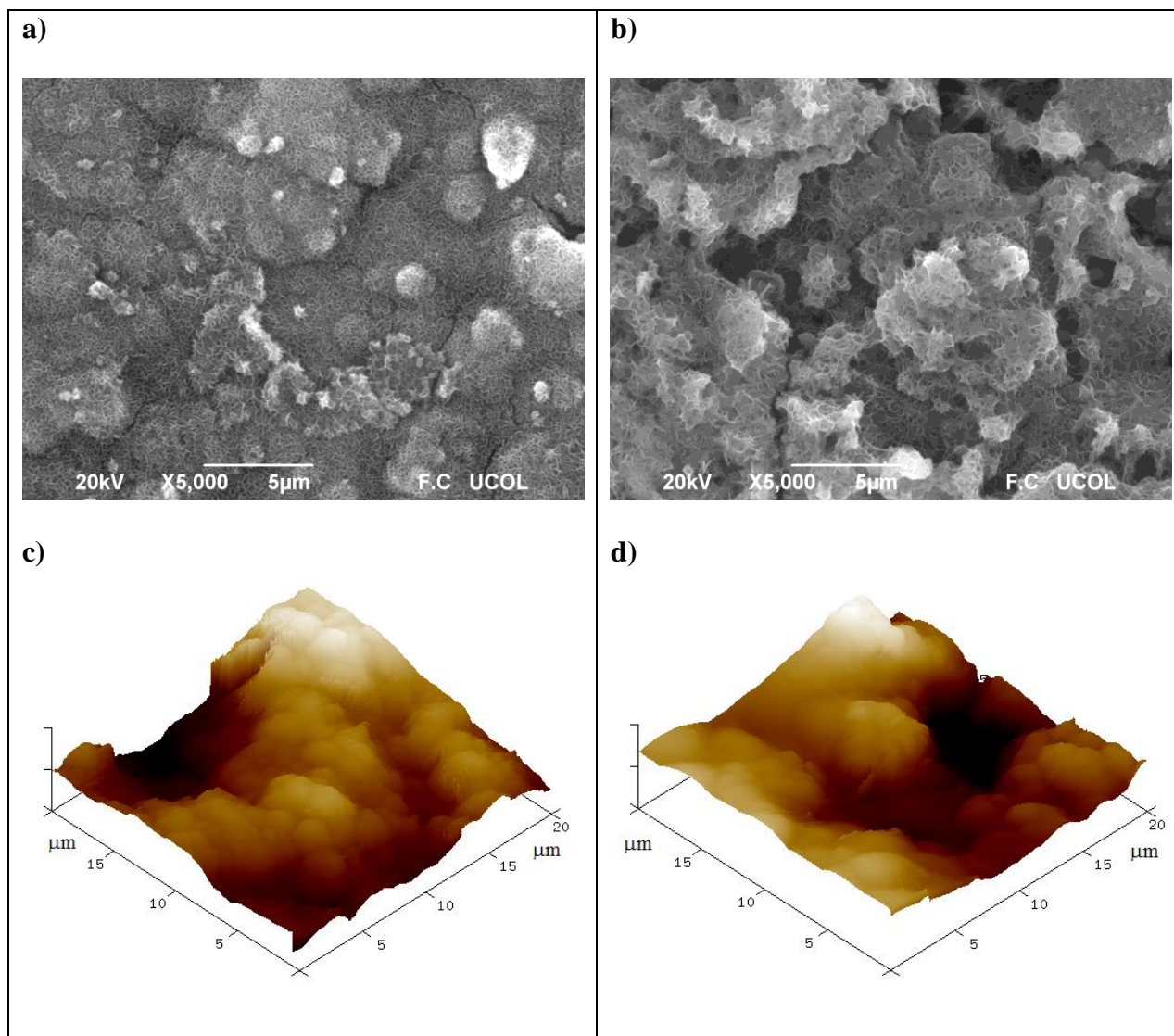


**Figure 5.** SEM and AFM micrographs of PPy  $0.1\ \text{mol L}^{-1}$  in  $\text{KNO}_3$  synthesized by cyclic voltammetry on CS-1018: a) and c) untreated (NT), b) and d) treated (T) in 10%  $\text{HNO}_3$ . (40 cycles,  $100\ \text{mVs}^{-1}$ ).

Figure 6a shows the scanning electron micrograph of the PPy deposit in potassium nitrate medium on CS-1018 NT, using as synthesis technique the imposition of a constant value of potential. The deposit obtained was irregular, with small cracked areas and weakly adhered to the substrate.

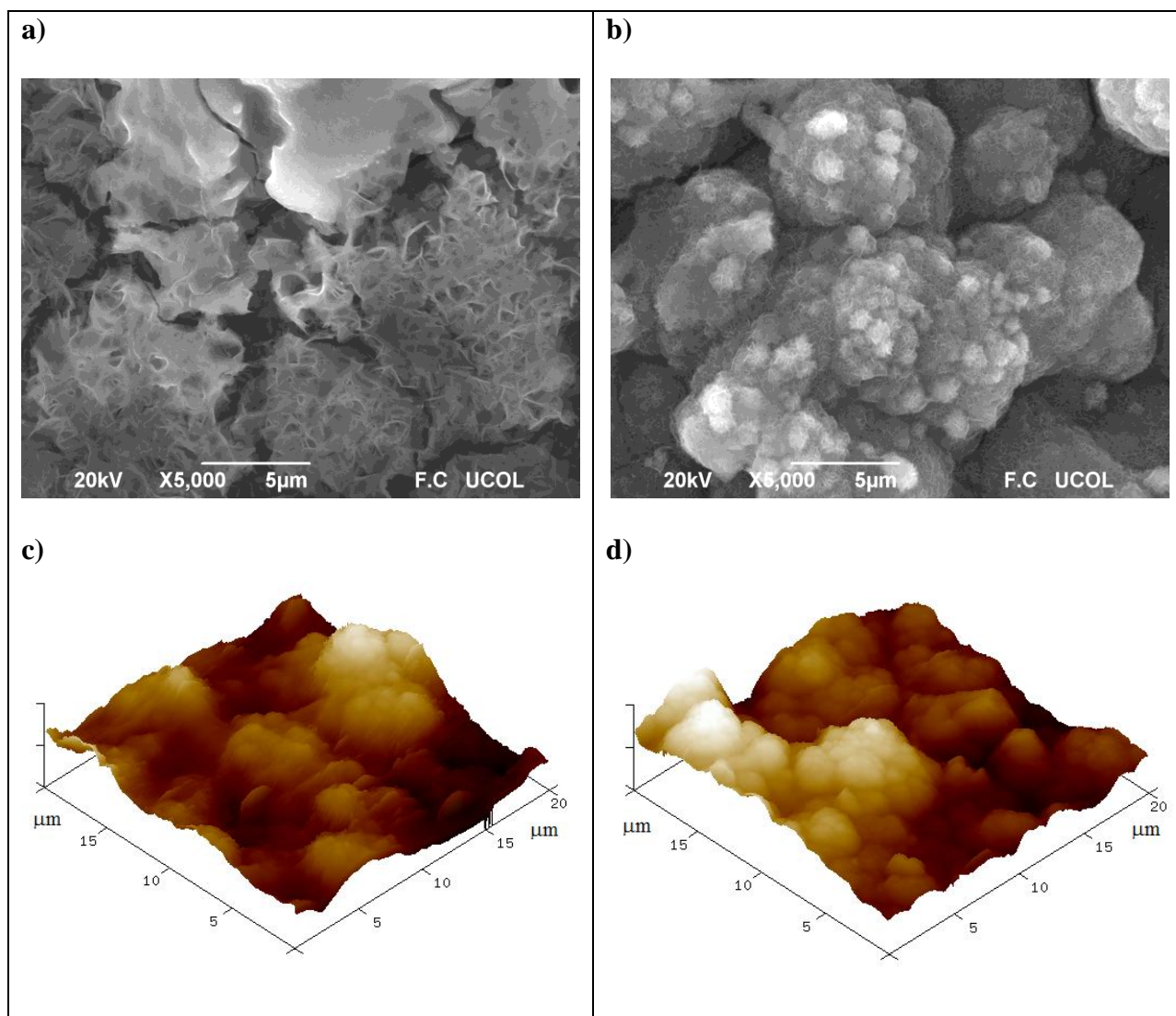


**Figure 6.** SEM and AFM micrographs of the PPy deposit by the chronoamperometry technique on CS-1018, in  $\text{KNO}_3$  with  $0.1 \text{ mol L}^{-1}$  Py: a) and c) untreated (NT), b) and d) treated (T) in 10%  $\text{HNO}_3$ .

The PPy deposit on the CS-1018 T synthesized with CA technique showed greater instability, identified by areas of detached PPy (Figure 6b). Figure 6c shows an irregular PPy film (on CS-1018 NT), reaching a maximum height of  $3.95 \mu\text{m}$ . The film shows circular clusters, with no specific arrangement with surface dimensions ranging from  $1.74 \mu\text{m}^2$  to  $6.65 \mu\text{m}^2$ . According to the agglomerations size it is safe to say that it is not such a thick layer deposited on the substrate, having a roughness of  $0.69 \mu\text{m}$ .

The PPy deposit on CS-1018 T is shown in Figure 6d, where a film with irregular more pronounced clumps and nodules with surface areas ranging between  $5.77 \mu\text{m}^2$  and  $19.88 \mu\text{m}^2$ , with a difference between the highest region and the deepest region of  $5.63 \mu\text{m}$  and a roughness of  $0.87 \mu\text{m}$ . The results shown in Figures 5 and 6 indicate that the synthesis technique plays an important role in the final film morphology. Using as dopant the anion  $\text{NO}_3^-$ , the obtained PPy film by using cyclic voltammetry technique has better adhesion-stability properties.



After characterization by SEM and AFM, we proceeded to study the electrochemical stability of PPy on the CS-1018 substrate. The stability test consisted of applying 500 cycles of charge/discharge at a scan rate of  $500 \text{ mVs}^{-1}$ , in  $0.1 \text{ mol L}^{-1}$  KCl aqueous solution. This process of charge/discharge generates a contraction/expansion movement of the deposited polymer, degrading and affecting its physical, chemical and electrochemical properties. After 500 cycles of potential a cyclic voltammetry at  $100 \text{ mVs}^{-1}$  is performed in  $0.1 \text{ mol L}^{-1}$  KCl solution and comparing the areas under the curve can be quantified the PPy that remained deposited on the CS-1018 [31].

Figure 7 shows the electrochemical characterization of deposited PPy on CS-1018 NT synthesized by the chronoamperometry technique, where it is observed that the polymer becomes unstable after the charging/discharging process because the area decreased ( $a = 0.0117 \text{ C}$ ) compared to the area of the deposit before the stability test ( $a = 0.0273 \text{ C}$ ).

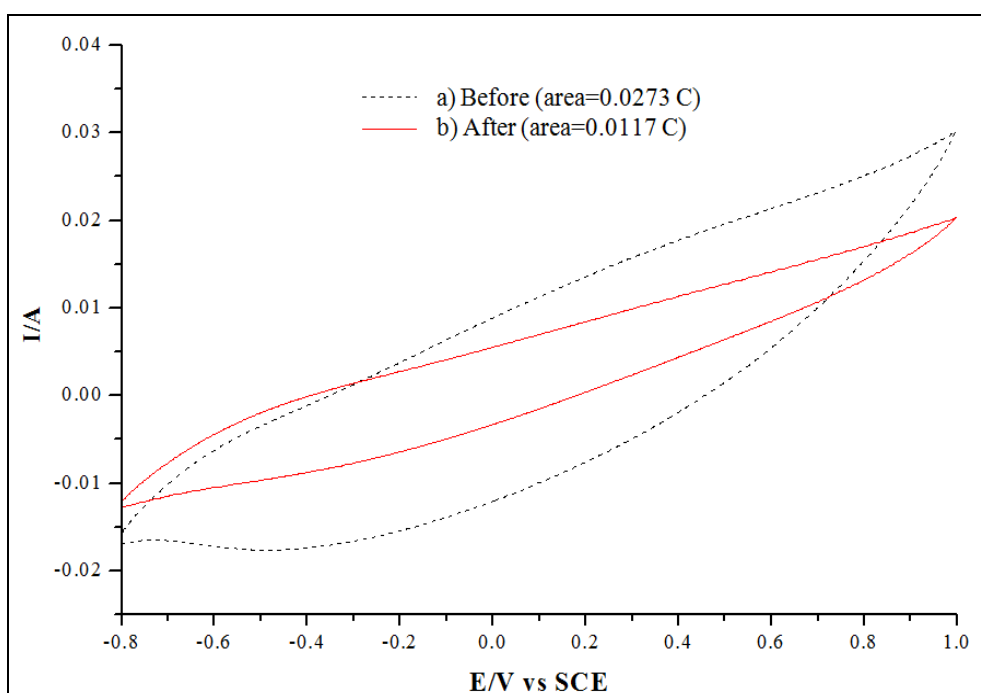


**Figure 7.** Evaluation of electrochemical deposition of PPy in  $0.1 \text{ mol L}^{-1}$   $\text{KNO}_3$  obtained by the chronoamperometry technique on CS-1018 NT (before and after the stability test).

The materials formed by both techniques show a decrease of the electrochemical signal after the accelerated stability test, so it is proposed that there may be two possibilities: deactivation (passivation state) or the physical detachment of the material.

### 3.4. EDX elemental characterization

In order to analyze the elemental composition of the obtained PPy deposit. A spectroscopic dispersive X-ray energy (EDX) was performed. An EDX of CS-1018 was conducted as a reference for comparison (not shown). In the spectrum with the characteristic signals of iron (0.70, 6.39 and 7 keV)

and carbon (0.27 keV) are observed. The spectrum of the electrodeposited PPy by cyclic voltammetry on CS-1018 NT in electrolytic nitrate medium is shown in Figure 8, which shows signals characteristic of the elements present in the sample; it is observed that the iron and oxygen signals are greater after the stability test; however the carbon and nitrogen signals (elements of the polymer chain) decreased.

In Figure 8, it is observed that the carbon signal before stability test, due to PPy formed, is higher compared to the signal after the test. That is, the deposit degrades after the test. An increase was also observed in the iron signals, which is the base element of the electrode, this confirms the hypothesis about the polymer degradation.

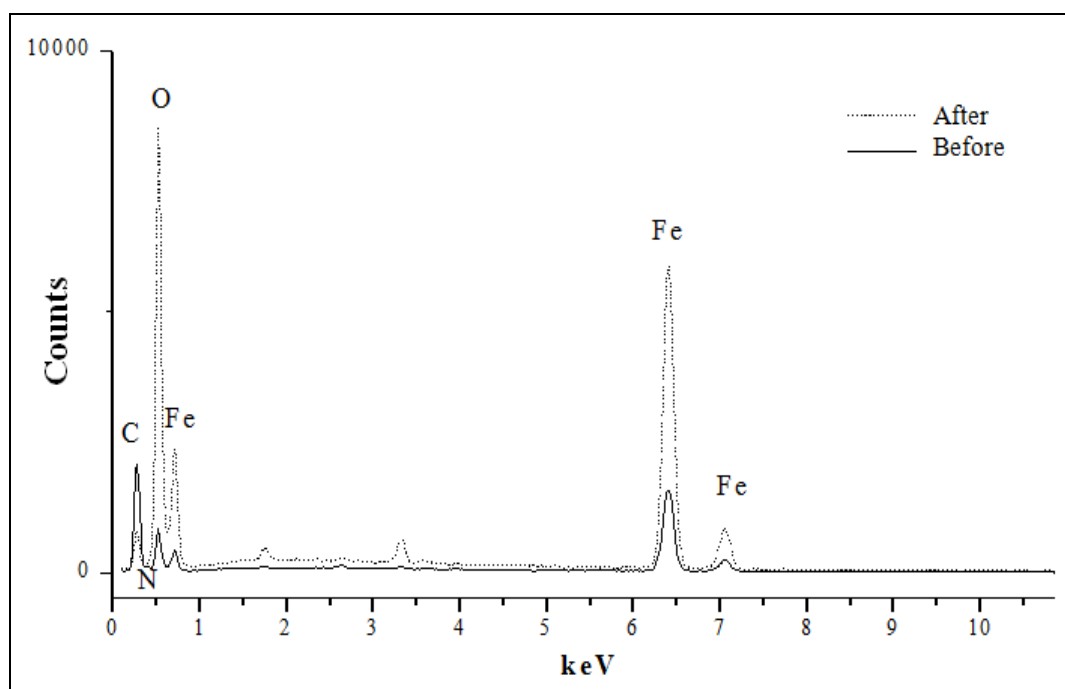


**Figure 8.** EDX spectra of PPy electrodeposited on CS-1018 NT, obtained by cyclic voltammetry (before and after the stability test).

The values of elemental composition of the deposits before and after the stability test are shown in Table 1. It's important to say that the electron beam emitted to the sample by SEM-EDX reaches a depth range of up to 5  $\mu\text{m}$  so that the analysis detects the CS-1018 iron because the thickness of the deposited polymer is close to this value. The percentage of iron is increased after the stability test, which is indicative of two things: the reduction of the thickness of the deposited polymer and the possible opening of the polymer structure (high porosity) [33].

After the stability test, the polymer undergoes a process of wear down and/or rearrangement in its structure this degradation/oxidation is noticeable in the decrease of percentage weight of carbon and nitrogen and an increase of oxygen and iron [34], shown in Table 1. Due to oxidation of the steel and the consequent formation of FeO and/or Fe<sub>2</sub>O<sub>3</sub>.

**Table 1.** Composition of deposit obtained on CS-1018 NT by cyclic voltammetry (before and after the stability test).

Component	Weight before/ (%)	Weight after/ (%)	Weight change/ (%)
<b>C</b>	47.88	10.83	77.4
<b>N</b>	5.45	3.17	41.8
<b>Fe</b>	26.81	43.35	-61.7
<b>O</b>	19.86	40.59	-118.3

Similarly a stability study was performed to the PPy deposit formed on CS-1018 T synthesized by cyclic voltammetry. In Table 2, is shown that the percentages of carbon and nitrogen also decrease after the stability test, as well as the membrane synthesized by chronoamperometry. In a similar way the Fe and O percentages are increased due to a partial destruction of the polymer. These results show that although the electrodeposition technique has an influence on the conductivity and electroactivity of the polymer, also governs the properties of the final polymer, such as: morphology, chemical and electrochemical stability [35].

**Table 2.** Composition of deposit obtained on CS-1018 treated in 10% HNO<sub>3</sub> by cyclic voltammetry (before and after stability test).

Component	Weight before/ (%)	Weight after/ (%)	Weight change/ (%)
<b>C</b>	35.24	6.28	82.2
<b>N</b>	5.34	2.81	47.4
<b>Fe</b>	25.25	48.96	-93.9
<b>O</b>	32.16	39.11	-21.6

Table 3 shows the elemental composition of the deposits of PPy on CS-1018 NT using KNO<sub>3</sub> as electrolyte when CA technique is used. It is observed that a weight percentage of carbon and nitrogen decrease considerably after the stability tests. Meanwhile iron and oxygen increased after the stability test. This reveals an unstable electrochemically film by the wear down process and rearrangement in their structure, which coincides with the electrochemical results shown previously.

**Table 3.** Composition of the deposit obtained on CS-1018 NT by chronoamperometry (before and after stability test).

Component	Weight before/ (%)	Weight after/ (%)	Weight change/ (%)
<b>C</b>	29.62	8.59	71.0
<b>N</b>	5.36	3.45	35.6
<b>Fe</b>	31.01	41.47	-33.7
<b>O</b>	32.5	44.09	-35.7

Table 4 shows the elemental composition taken from the EDX spectrum for a PPy deposit on CS-1018 T, where a similar behavior is observed on the CS-1018 untreated NT but with more pronounced differences of weight percent of carbon and iron before and after the stability test.

**Table 4.** Composition of the PPy deposit obtained on CS-1018 T by chronoamperometry (before and after electrochemical stability test).

Component	Weight before/ (%)	Weight after/ (%)	Weight change/ (%)
<b>C</b>	41.25	9.15	77.8
<b>N</b>	2.62	3.83	-46.2
<b>Fe</b>	19.96	42.16	-111.2
<b>O</b>	33.76	40.89	-21.1

### 3.5. Contact angle characterization of the PPy surface

The values of the contact angle studies of the metal surface with and without treatment are shown in Table 5, also the values obtained with the respective polypyrrole deposits with both water and crude oil. It is observed that the contact angle of the surface of CS-1018 NT is 70° with water and crude oil. In other words, the metal surface without treatment has the same affinity for both. When the steel surface is treated, CS-1018 T, the contact angle with water is 110°. So we can say that the treatment with nitric acid gives a slightly hydrophobic behavior; on the other hand, the contact angle also increases with crude and remains at a value close to 90° that is the limit between the oleophilic/oleophobic balances. The contact angle results show that the acid treatment to the metal surface gives hydrophobic properties to the surface, which is in agreement with the results of AFM showing rougher metal surfaces in acidic medium. These trends are consistent with those reported in the literature [28, 29, 36, 37].

Meanwhile polymer deposits made on CS-1018 T generated rougher surfaces than those synthesized on CS-1018 NT. In both cases, after the synthesis of the PPy coating, the water contact angle increases as the surface roughness increases. Depositing PPy on CS-1018 NT has a slightly hydrophilic behavior contrary to the presenting when the polymer is synthesized on a treated surface.

The contact angle values with crude follow the same trend as water. This value is lower in the untreated surface, which appears to be an area of lower roughness. However, the values in the presence of the polymer coating are very similar and close to 90°, the threshold value to determine the oleophilic nature of the surface.

The values show that the surface CS-1018 T PPy-KNO<sub>3</sub> forms a contact angle greater than the surface CS-1018 NT PPy-KNO<sub>3</sub>. That is, that the higher the porosity of the metal surface, a higher roughness of the polymer deposited is obtained and in consequence decreases the polypyrrole-oil interaction.

**Table 5.** Values of water contact angle with the selected deposits.

Sample	Contact angle/(°)	
	Water	Oil
CS-1018 NT	70	70
CS-1018 T	110	85
PPy-KNO <sub>3</sub> on CS-1018 NT, CV	80	83
PPy-KNO <sub>3</sub> on CS-1018 T, CV	125	90

#### 4. CONCLUSIONS

Pretreatment of CS-1018 with 10% HNO<sub>3</sub> did not influence the deposition of PPy on CS-1018, however, it influenced the morphology of the formed PPy, creating uneven surfaces. Regarding stability and adhesion of the deposits on the CS-1018, PPy deposits showed no significant variation before and after the stability test. Most EDS showed decreased carbon and nitrogen and increased iron and oxygen after the stability test CS-1018 untreated and treated in HNO<sub>3</sub> due to polymer degradation process. The materials that showed better electrochemical, morphological, and spectroscopic properties for application of interest were the PPy deposited with KNO<sub>3</sub> in CS-1018 untreated and treated in HNO<sub>3</sub> with the technique of cyclic voltammetry. The water's contact angle with CS-1018 untreated was less than 90° (hydrophilic) and the CS-1018 treated in HNO<sub>3</sub> was greater than 90° (hydrophobic). The contact angle with crude oil was influenced by the roughness of the polymer film. As increased roughness, increased contact angle. More efficiently the material to inhibit the deposition of asphaltenes deposition was PPy-KNO<sub>3</sub>, treated in HNO<sub>3</sub>, cyclic voltammetry, an angle of 90° between the PPy film and the oil drop.

#### ACKNOWLEDGMENTS

O.E. Vázquez-Noriega acknowledges the scholarship granted by CONACYT-Mexico. We acknowledge the funding through CONACyT-Mexico projects No: 177480, 224366 and ProIFOPEP DGEST-Mexico project No: 4514.12-P, and the Fis. D. Pozas of the University of Colima for the study of SEM-EDS microscopy.

#### References

1. S. M. Richardson and H. Y. McSween, *Geochemistry: Pathways and Processes*, Prentice-Hall, New York (1989).
2. P. Luo, X. Wan, Y. Gu, H. Zhang and S. Moghadam, "Asphaltene precipitation and its effects on the vapour extraction (VAPEX) heavy oil recovery process", *Society of Petroleum Engineers (SPE)*, Alberta, Canada, (2008) 314.

3. T. A. Al-Sahhaf, M. A. Fahim and A. S. Elkilani, *Fluid Phase Equilib.*, 194 (2002) 1047.
4. K. J. Leontaritis and G. A. Mansoori, *J. Petr. Sci. Eng.* 1 (1988) 229.
5. E. Rogel, T. Miao, J. Vien and M. Roye, *Fuel*, 147 (2015) 155.
6. S. R. Panuganti, F. M. Vargas, D. L. Gonzalez, A. S. Kurup and W. G. Chapman, *Fuel*, 93 (2012) 658.
7. A. C. Afghoul, S. Amaravadi, A. Boumali, J. C. N. Calmeto, J. Lima, J. Lovell, S. Tinkham, K. Zmlak and T. Stall, *Schlumberger Oilfield Review*, 16 (2004) 38.
8. P. S. Kumar, S. V. Gisberger, J. Harris, E. Ferdiansyah, M. Brady, S. A. Harthy and A. Pandey, *SPE Production & Operations*, 23 (2008) 119.
9. W. Frenier, M. Ziauddin, and R. Venkatesan, *Organic Deposits in Oil and Gas Production*, Society of Petroleum Engineers, Texas, (2010).
10. S. J. Park and G. A. Mansoori, *Energy Sources*, 10 (1988) 109.
11. L. C. Rocha, M. Silva and A. C. da Silva, *J. Petr. Sci. Eng.* 51 (2006) 26.
12. O. Castellano, R. Gimón and H. Soscun, *Energy & fuels*, 25 (2011) 2526.
13. J. I. Martins, M. Bazzaoui, T. C. Reis, E. A. Bazzaoui and L. Martins, *Synt. Met.*, 129 (2002) 221.
14. F. Beck and R. Michaelis, *J. Coat. Tech.* 64 (1992) 59.
15. U. Paramo-Garcia, N. Batina and J. G. Ibanez, *Int. J. Electrochem. Sci.*, 7 (2012) 12316.
16. U. Páramo-Garcia, J. G. Ibanez and N. Batina, *Int. J. Electrochem. Sci.*, 8 (2013) 2656.
17. L. F. Warren and D. P. Anderson, *J. Electrochem. Soc.*, 134 (1987) 101.
18. W. Su and J. O. Iroh, *Synt. Met.*, 114 (2000) 225.
19. T. Patois, B. Lakard, S. Monney, X. Roizard and P. Fievet, *Synt. Met.*, 161 (2011) 2498.
20. M. B. González and S. B. Saidman, *Prog. Org. Coat.*, 78 (2015) 21.
21. W. Su and J. O. Iroh, *Electrochim. Acta*, 44 (1999) 4655.
22. A. Mollahosseini and E. Noroozian, *Synt. Met.*, 159 (2009) 1247.
23. D. Kowalski, M. Ueda and T. Ohtsuka, *Corr. Sci.*, 49 (2007) 3442.
24. D. E. Tallman, G. M. Spinks, A. J. Dominis and G. G. Wallace, *J. Sol. St. Electrochem.*, 6 (2002) 73.
25. G. M. Spinks, A. J. Dominis, G. G. Wallace and D. E. Tallman, *J. Sol. St. Electrochem.*, 6 (2002) 85.
26. R. John and G. G. Wallace, *J. Electroanal. Chem. Int. Electrochem.*, 306 (1991) 157.
27. D. J. Fermin, J. Mostany and B. R. Scharifker, *Curr. Topics Electrochem.*, 2 (1993) 2147.
28. W. Su and J. O. Iroh, *Electrochim. Acta*, 46 (2000) 1.
29. Y. Wang and D. O. Northwood, *Thin Sol. Films*, 516 (2008) 7427.
30. Y. Wang and K. Rajeshwar, *J. Electroanal. Chem.*, 425 (1997) 183.
31. I. J. Lehr and B. S. Saidman, *Synt. Met.*, 159 (2009) 522.
32. R. A. Khalkhali, W. E. Price and G. G. Wallace, *Reac. Func. Pol.*, 56 (2003) 141.
33. J. Goldstein, D. Newbury and D. Joy, *Scanning Electron Microscopy and X-Ray Microanalysis*, Springer (2002).
34. P. A. Mabrouk, *Synt. Met.*, 150 (2005) 101.
35. L. Feng, S. Li, Y. Li, H. Li, L. Zhang, J. Zhai, Y. Song, B. Liu, L. Jiang and D. Zhu, *Adv. Mat.*, 14 (2002) 1857.
36. A. Lafuma and D. Quéré, *Nat. Mat.*, 2 (2003) 457.
37. R. G. dos Santos, R. S. Mohamed, A. C. Bannwart and W. Loh, *J. Petr. Sci. Eng.*, 121 (2014) 66.